Energy production potential and economic viability of grid-connected wind/PV systems at Saudi Arabian coastal areas

Makbul A. M. Ramli, Ssennoga Twaha, and Abdulaziz U. Alghamdi

Citation: Journal of Renewable and Sustainable Energy **9**, 065910 (2017);
View online: https://doi.org/10.1063/1.5005597
View Table of Contents: http://aip.scitation.org/toc/rse/9/6
Published by the American Institute of Physics

Energy production potential and economic viability of grid-connected wind/PV systems at Saudi Arabian coastal areas

Makbul A. M. Ramli,[1,a)] Ssennoga Twaha,[2,a)] and Abdulaziz U. Alghamdi[1]
[1]*Department of Electrical and Computer Engineering, King Abdulaziz University, Jeddah 21589, Saudi Arabia*
[2]*Energy and Sustainability Division, Faculty of Engineering, University of Nottingham, Nottingham NG7 2RD, United Kingdom*

(Received 19 September 2017; accepted 7 December 2017; published online 27 December 2017)

This paper analyzes the electricity production potential and economic viability of grid-connected wind/photovoltaic (PV) energy systems at two coastal cities, Yanbu and Dhahran in Saudi Arabia. First, wind energy is assessed based on the hourly wind speed observation data recorded over the entire year 2013 in the selected locations. Electricity generation potential is estimated using two wind turbines: Vestas V82 and V90 models. The results indicate that both locations have sufficient wind resources for wind turbine operation. Strong wind resources are more common at Dhahran than at Yanbu with wind speeds above 3.5 m/s, accounting for 60.12% of the wind data at Dhahran, which is higher than 51.2% of Yanbu. Grid-connected hybrid systems using Vestas V90 wind turbines had the highest net present cost (NPC) compared with other configurations. The inclusion of battery storage units slightly increases the NPC. Surprisingly, systems with the highest NPC produced the least electricity. In contrast, cheaper V82-based systems had the lowest NPC and levelized cost of energy and produced the most electricity. Hence, a grid-connected wind/PV system using V82 turbines is most economically viable. Incorporating a small battery storage unit in the systems minimizes capacity shortages and improves reliability at minimal extra cost. Using different wind turbines with a lower cut-in speed of 3 m/s could increase the electricity production, as 9.1% and 10.3% of wind observations at Yanbu and Dhahran, respectively, had a wind speed of 3 m/s. *Published by AIP Publishing.* https://doi.org/10.1063/1.5005597

I. INTRODUCTION

Interest in clean energy technology and sustainable development has increased worldwide over the last decade, mainly due to the challenges of climate change. However, the world's energy resources are unevenly distributed, and energy consumption is increasing at a greater rate than the human population.[1] Globally, some 1.3 billion people have no access to electricity.[2] In recent years, increasing rates of air pollution and uncertainty of future oil prices have stimulated global interest in the use of hybrid power stations.[3] Saudi Arabia has the highest electrical energy consumption among the Gulf Cooperation Council (GCC) countries. The peak electricity demand is predicted to reach 60 GW by 2023, which will stimulate energy investment.[4] Therefore, there is a pressing need for sustainable energy development in the country. Numerous efforts have been made to utilize renewable energy resources such as solar and wind to complement the fossil fuel based generated power.[5]

Since Saudi Arabia mainly uses fossil fuels for electricity production, it emits high amounts of carbon dioxide to the atmosphere, which contributes to global warming. The increasing rate of carbon emissions in Saudi Arabia is mainly attributed to rapid development and industrialization, especially electricity generation for the increasing numbers of people.[6] Global warming

[a)]Authors to whom correspondence should be addressed: mramli@kau.edu.sa and ssennogatwaha2007@gmail.com

concerns have increased the need for technologies that have a relatively low environmental impact.[7,8] Carbon capture technology, carbon emission-constrained dispatch, and renewable energy generation systems are among the three most-suggested methods for reducing CO_2 production. The best solution is to generate energy from renewable resources such as wind, solar, hydro, and geothermal, instead of exhausting fossil fuels. Renewable resources are attractive to many energy-based economics due to the need to reduce greenhouse gas emissions and increase electric energy security and because of the high cost of ever diminishing fossil fuels.[9] Therefore, future renewable energy power plants need to be developed in order to reduce the environmental impacts of limited fossil fuel resources.[10]

As a result of continuous improvement in utility restructuring and power deregulation, interest in distributed generation (DG) applications has increased significantly.[11] The DG concept is to locate small-scale power generators close to electricity customers.[12] It generally uses a combination of renewable and conventional energy resources to achieve combined heat and power (CHP) generation. In power generation applications, DG can be arranged as standalone or grid-connected systems. However, because of the disadvantages of standalone systems (e.g., the stochastic nature of wind energy and solar energy[13]), hybrid systems are preferable. Energy from one source, such as wind, can compensate for shortages of energy from other sources such as solar. However, for comprehensive system evaluation, it is necessary to accurately assess the energy resources in terms of potential, technical requirements, and economic viability before systems are implemented. For example, it is necessary to evaluate the wind speed and direction, solar irradiation, and the expected electricity output from different types of wind turbines. The scale of surpluses and shortages may also be evaluated.[14]

Various studies have been carried out to design and analyze hybrid DG systems by employing a range of modeling tools. A review of recent trends in optimization techniques for solar photovoltaic/wind hybrid energy systems was carried out in which various techniques used for the optimization of renewable based hybrid energy systems were analyzed including PV/wind hybrid system sizing methods.[15] The need for improving the reliability of the photovoltaic-based hybrid power system with battery storage in low wind locations is studied using Hybrid Optimization of Multiple Energy Resources (HOMER) software.[16] Qolipour *et al.* conducted a techno–economic analysis of small wind turbines in Iran. Six areas within Ardabil province were ranked by a hybrid approach composed of Game Theory, Balanced Scorecard, and Data Envelopment Analysis.[17] The authors in Ref. 18 carried out a technical and economic evaluation of hybrid PV/wind systems in onshore, remote areas of Indonesia. It has been demonstrated that batteries and wind turbines are the most important components of hybrid systems. Although expensive, these systems can provide energy during the night. It is, therefore, suggested that system size is carefully considered in order to minimize cost while ensuring that load demands are met. A techno-economic analysis was done for a standalone PV/wind/diesel/battery hybrid system in Abu Dhabi.[19] It was designed to produce loads of 500 kW, 1 MW, and 5 MW to fulfill the primary load for 250, 500, and 2500 households, respectively. The CO_2 emitted by the 500 kW optimal hybrid system was 37% lower than a conventional diesel generator-only system. The feasibility study was carried out by analyzing wind speed data for the period 2008–2014 using HOMER software. A feasibility study of small hydro/PV/wind hybrid electric generators was conducted at six sites with small-scale hydropower potential.[20] Another study investigated the potential to integrate renewable energy resources for trigeneration applications for a remote island community.[14]

In 2010, Hafez and Bhattacharya designed hybrid microgrid systems for various configurations.[21] They considered fully renewable, diesel-only, hybrid renewable/diesel, and external grid-connected systems and estimated their environmental emissions, operational performance, and economics. In addition, a comparison of different hybrid generation systems in terms of net present cost (NPC), levelized cost of energy (LCOE), and renewable energy penetration (REP) was made. A feasibility study was conducted on a standalone hybrid solar/wind energy system in Ethiopia, in which the influences of wind speed, PV cost, and diesel prices were analyzed with sensitivity diagrams to find optimal solutions.[22] Another study investigated the performance of a hybrid PV/wind/diesel/battery configuration based on hourly measurements of solar

radiation, ambient temperature, and wind speed over a one year period in Southern Algeria,[23] while a study of a wind/diesel hybrid system was presented in Ref. 24. The proposed hybrid system was optimized using HOMER, taking into account renewable resource potential and energy demands while maximizing renewable electricity use and fuel savings. Similarly, a wind power potential assessment was performed for five locations in Algeria using nine types of small and medium wind turbines from five manufacturers. It concluded that most of these turbines produced approximately 1000–10 000 MWh of electricity per year at 60 m of altitude and could easily satisfy electricity requirements for irrigation and households in rural and arid regions. In our previous research, we designed a grid-connected PV system. Our analysis indicated that it could serve as a viable alternative to the diesel generators which had been used to supplement a hydro-power system.[25] Electricity could be sold back to the grid through a net metering system when the PV system generated surplus energy. This could help to fully utilize the abundant renewable energy resources available in the country.[26]

Of particular interest are the several studies that have been carried out on the implementation of renewable resources in Saudi Arabia. The performance evaluation of small wind turbines for off-grid applications in Saudi Arabia was done, whereby the energy output and plant capacity factor (PCF) of small wind turbines rated powers in the range of 1–3 kW, 5–10 kW, 15–20 kW, and 50–80 kW were studied.[27] Suitable hub heights for different load requirements and applications were recommended. The wind data used were obtained from the Juaymah meteorological station for the year 2006. Other researchers have presented the wind characteristics and resource assessment of the Jubail industrial city using measured hourly mean wind speed data at 10, 50, and 90 m above the ground level from 2008 to 2012.[28] The comparison of energy output from the selected wind turbines with power ratings ranging from 1.8 to 3.3 MW showed that the most efficient wind turbine was one with a rated power of 3 MW. Another study evaluated the use of wind power for pumping water to areas located far from the national grid. Micro-turbines with a power capacity in the range of 1 to 10 kW with Goulds 45 J type water pumps were selected to generate wind energy and pump water in the Rawdat Ben Habbas, Arar, and Juaymah areas.[29] Wind speed data and available energy in the Rafha area were analyzed using wind machines of 600, 1000, and 1500 kW sizes, where long-term annual mean values of wind speed were found to vary between a minimum of 2.5 m/s and a maximum of 4.9 m/s.[30]

A comparison was made among hybrid renewable energy systems in Saudi Arabia whereby three hybrid systems were compared with respect to their cost per unit energy.[31] The connection of the system to the grid reduced the system cost because the cost of energy storage decreased. A previous study[32] discussed a hybrid PV/diesel/battery system for a remote village in the northeastern region of the country. It concluded that the hybrid system was more cost-effective than a standalone diesel system. Several studies on global solar radiation have been carried out for different regions in Saudi Arabia, including the most suitable locations for solar energy applications.[33,34] Some 35 solar resource monitoring stations have been installed throughout the country for the collection of high-quality data on solar resources.[35]

The development of wind- and solar-based power systems requires high quality wind and solar data. These aid energy exploration projects to conduct feasibility studies. To allow efficient collection of renewable resources that are widely dispersed (wind, sun, etc.), the optimal sizing of hybrid renewable power generation systems is essential.[36] In this paper, the energy production potential and economic viability of grid-connected wind/PV hybrid energy systems are assessed. Comparative analysis is carried out for two Saudi Arabian coastal areas: Yanbu and Dhahran. The study is based on wind and solar data from the year 2013. First, the energy potential of wind is assessed in terms of wind speed using wind rose plots generated with WindRose Pro software. Electrical energy generation potential from wind and solar resources is evaluated, and economic analyses are then carried out using HOMER software. The rest of the paper is organized as follows: Sec. II summarizes wind and solar characteristics for the selected locations. Section III discusses methods and tools used. Section IV details the component specifications and model inputs. In Sec. V, results are presented and discussed, while concluding remarks are made in Sec. VI.

II. WIND AND SOLAR RESOURCES AT THE STUDY SITES

A. Background of Yanbu and Dhahran

In this study, two coastal cities, Yanbu and Dhahran, were selected as the study sites. Wind and solar data obtained from GIS[37] were used to characterize the wind and solar resources of Yanbu and Dhahran. Yanbu is located in Al Madinah province, western Saudi Arabia (24.0232° N, 38.1900° E), while Dhahran is located in Eastern Province, near Bahrain (26.2361° N, 50.0393° E; Fig. 1).

A total of 8761 hourly wind and solar observations were used. The wind data consisted of wind speed, direction, and temperature, recorded hourly throughout 2013.

B. Wind data characteristics

1. Wind data statistical features

Table I summarizes the wind data for Yanbu and Dhahran. Wind speeds ranged from 0 to 11 m/s in Yanbu and 0 to 13 m/s in Dhahran, with means of 3.8 and 4.3 m/s, respectively. Standard deviations were similar (2.035 and 2.025 m/s, respectively). Figures 2(a) and 2(b) show the hourly wind speed distributions for Yanbu and Dhahran, respectively. It is clear from these figures that wind speed is variable in both locations—sometimes, they are very low, while other times, they are high.

2. Comparison of average seasonal and diurnal wind speeds

Figure 3 shows the seasonal variation in wind speed at Yanbu and Dhahran. Wind speeds between January and June were higher in Dhahran than in Yanbu. Dhahran's maximum speed of 5.77 m/s occurred in June. From July to September, there were higher wind speeds in Yanbu than in Dhahran. Yanbu's maximum wind speed of 4.82 m/s occurred in July. From October

FIG. 1. Location of Yanbu and Dhahran, Saudi Arabia.

TABLE I. Summary of annual wind data at the study sites (m/s).

	Yanbu	Dhahran
Min	0	0
Max	10	13
Average	3.8	4.2
Standard deviation	2.035	2.025
Variance	4.143	4.099
Mode	3.7	3.3

through December, wind speeds were again higher in Dhahran. Both locations experienced their lowest wind speeds in November, at 3.06 m/s and 3.55 m/s for Yanbu and Dhahran, respectively. These values are similar to the estimates reported for Dhahran[38] and the measured values for Jubail, which is situated near Dhahran.[28] Figure 4 shows the diurnal hourly average wind speed variation at both locations. The maximum average wind speeds occurred near midday—at 11:30 am and 12:30 pm for Yanbu and Dhahran, respectively. This is convenient as the electrical demand in Saudi Arabia peaks over the middle of the day. Morning wind speeds were higher in Dhahran than in Yanbu, with the lowest values occurring at approximately 9:30 am in Yanbu. In general, wind speeds in Dhahran were stronger than in Yanbu for most times of the

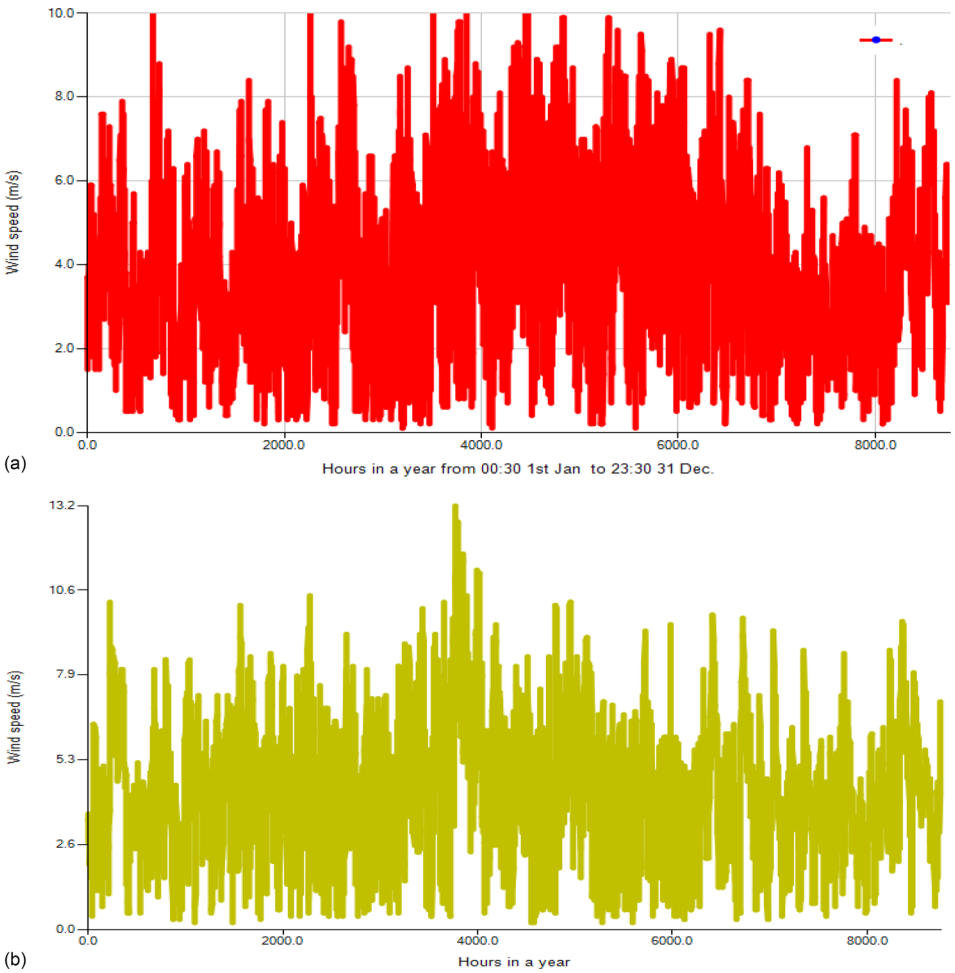

FIG. 2. (a) Hourly wind speed distribution over 2013 (Yanbu). (b) Hourly wind speed distribution over 2013 (Dhahran).

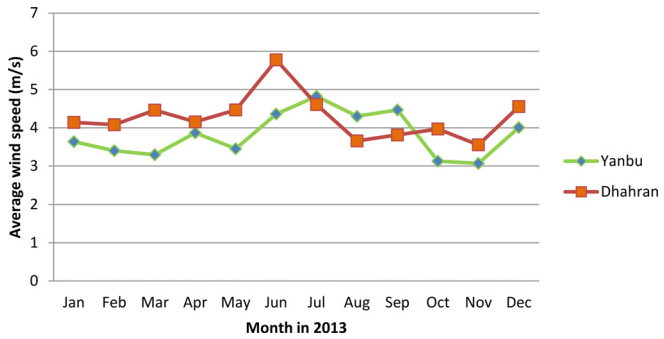

FIG. 3. Annual variation in average monthly wind speeds at the study sites.

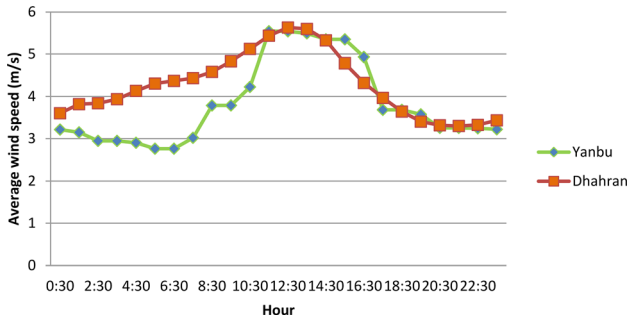

FIG. 4. Daily variation in average hourly wind speeds at the study sites.

day and seasons of the year. This means that more wind energy is available in Dhahran than in Yanbu although wind is still strong in Yanbu. Wind speed and direction frequencies will be discussed in Sec. V A.

C. Solar radiation and clearness index

Extra-terrestrial radiation on a horizontal surface is defined by

$$I_o = \frac{1}{\pi} I_{sc} \left(1 + 0.033 \cos \frac{360n}{365}\right) \cos \theta_z, \tag{1}$$

where n is the day of the year (1 to 365), θz is the zenith angle, and I_{SC} is the solar constant (1.367 kW/m^2).

The clearness index is the ratio of global horizontal radiation, I, to extraterrestrial horizontal radiation, I_o, and is expressed as

$$k = \frac{I}{I_o}. \tag{2}$$

Diffuse radiation on a horizontal surface as a function of the clearness index is given by

$$\frac{I_d}{I} = \begin{cases} 1 - 0.09k & \text{for } k \leq 0.22 \\ 0.9511 - 0.1604k + 4.388k^2 - 16.638k^3 + 12.336k^4 & \text{for } 0.22 < k \leq 0.80 \\ 0.165 & \text{for } k > 0.80. \end{cases} \tag{3}$$

Power output from a PV array is expressed as

$$P_{PV} = P_{PV,STC} f_{PV} f_{temp} \left(\frac{I_T}{I_{T,STC}}\right), \tag{4}$$

where $P_{PV,STC}$ is the rated capacity of the PV array under standard test conditions (kW), f_{PV} is the PV derating factor (%), I_T is the global solar radiation incident on the PV array (kW/m^2), $I_{T,STC}$ is the incident radiation at standard test conditions (1 kW/m^2), and f_{temp} is the temperature derating factor (dimensionless). The derating factor estimates reductions in PV array output due to dust on the panel surfaces, wiring losses, shading, aging, elevated temperature, or anything else that reduces the output of a PV array under ideal conditions.

Figures 5(a) and 5(b) show the seasonal radiation and clearness indexes for Dhahran and Yanbu. The maximum radiation received by Yanbu and Dhahran was about 5.978 and 5.605 kWh/m^2/day, respectively, which are enough to generate considerable power using PV arrays. Solar radiation was higher in Yanbu than in Dhahran.

III. METHODS AND TOOLS

WindRose Pro software was used to analyze the wind's speed and directional distribution. WindRose Pro software was used for analyzing and plotting directional variables. It can be used to represent wind roses and any other directional variables.[39] The spread of wind directions provides important information for wind turbine selection. A wind turbine with a horizontal axis can be faced towards the strongest wind speed direction in order to maximize energy harvesting.

The vertical extrapolation of wind speeds at the hub height for a given wind turbine is completed using two wind profile laws. The logarithmic law is defined as

$$v_2 = v_1 ln\left[\frac{h_2}{h_0}\right] \Big/ ln\left[\frac{h_1}{h_0}\right], \tag{5}$$

where v_2 is the wind speed in m/s at the hub height, v_1 is the wind speed in m/s at the anemometer height, h_2 is the hub height in m, h_1 is the anemometer height in m, and h_0 is the surface roughness in m.

The power law[40,41] is expressed as

$$v_2 = v_1 \left[\frac{h_2}{h_1}\right]^{\propto}, \tag{6}$$

where α is the wind shear exponent. The IEC standard specifies a wind shear exponent of 0.20 and 0.11 for normal (onshore) and extreme (onshore) wind conditions, respectively.

Having specified the hub height, the wind turbine power output can be taken from the power curve.[42,43]

The second tool used in this study is HOMER, a widely tested software package developed by the National Renewable Energy Laboratories and mainly used for the design and analysis of microgrid systems.[44] HOMER is optimization software for modeling and optimizing standalone and grid-connected microgrid systems and has been used by many studies around the world.[45–47] The simulation can give the NPC, total emission cost, LCOE, and REP for different system configurations. All possible system configurations are simulated, and the energy balance computations for each are performed based on ascending NPC.

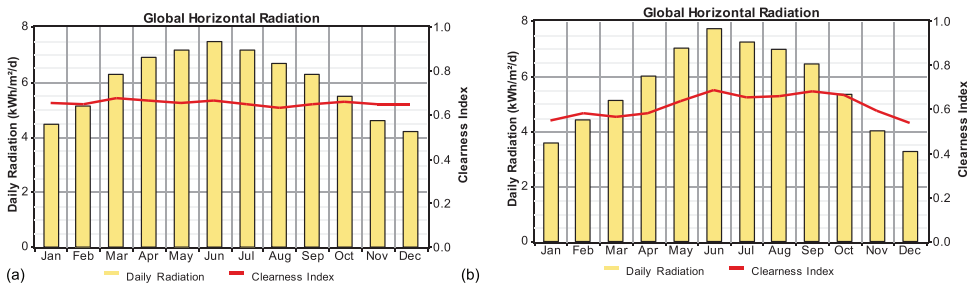

FIG. 5. (a) Mean monthly radiation and clearness index (Yanbu). (b) Mean monthly radiation and clearness index (Dhahran).

TABLE II. Technical and performance specifications of the wind turbines.

	Wind turbine type	
Parameter (units)	Vestas V82	Vestas V90
Anemometer height (m)	10	10
Hub height (m)	59	65
Roughness length (m)	0.0024	0.0024
Shear coefficient (-)	1.212955	1.224575
Average power density (W/m^2)	147.9438	120.5764
Standard deviation of power density (W/m^2)	213.7321	171.7205
Cut-out wind speed (m/s)	20	25
Rated wind speed (m/s)	13	15
Cut-in wind speed (m/s)	3.5	3.5
Rated wind power (kW)	1650	3000
Blade diameter (m)	82	90
Swept area (m^2)	5281	6362
Average wind speed (m/s)	5.179177	4.675896
Wind speed standard deviation (m/s)	2.456541	2.493491

IV. COMPONENT SPECIFICATIONS AND MODEL INPUTS

Technical and economic specifications for all components used in the simulations and the characteristics of wind turbines used in the analysis are as follows: Table II shows the technical and performance specifications of Vestas V82 and Vestas V90 wind turbines, which were selected for use in the analysis. The Vestas V90 model is a newer version than V82 and has a power rating of 3 MW, almost double that of V82 (1.65 MW). Both models have the same cut-in speed of 3.5 m/s but with different cut-out speeds—20 m/s and 25 m/s for V82 and V90, respectively. This means that the V90 model can survive at higher speed winds. However, V90 has a larger diameter and sweep area (90 m and 6362 m^2) compared to V82 (82 m and 5281 m^2). Therefore, V90 requires a larger construction area. Figure 6 shows the power curves for Vestas V82 and V90 wind turbines. The V90 model can generate more energy than V82 when both are operating at the same speed.

A load profile was generated with an average energy of 18 MW/day and a peak demand of 15 300 kW. Figure 7 shows the daily load profile for the cities under study. The residential load was assumed. The average electricity tariff in Saudi Arabia is 0.12 SR/kWh which is approximately US$0.032/kWh.[48] The "feed-in tariff" or sellback price for renewable energy has multiple rates—$0.022/kWh for the peak (1800–2400 h), $0.011/kWh for the shoulder (0600–1800 h), and

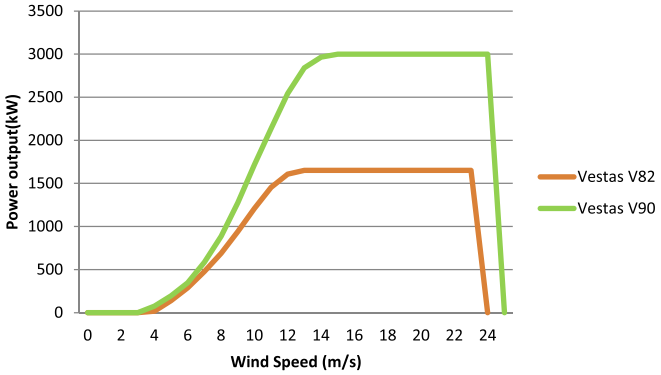

FIG. 6. Power curves of the wind turbines.

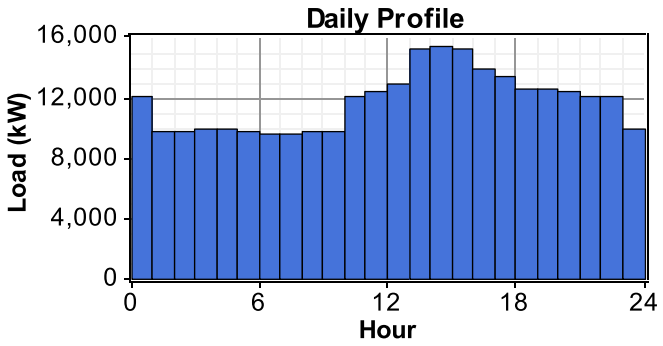

FIG. 7. Daily load profile.

\$0.009/kWh for the off-peak (0000–0600 h). The net supply of electricity to the grid (S_N) is equal to the electricity supplied to the grid (S_{GD}) minus electricity supplied by the grid (S_{GN}) and is expressed as[25]

$$S_N = S_{GD} - S_{GN}. \tag{7}$$

The real interest rate is equal to the nominal interest rate minus the inflation rate. In this study, an annual real interest rate of 0.6% was used. Table III shows the specifications of the

TABLE III. Specifications of components used in HOMER simulations.

Component	Specification	Description
PV array	Life	25 years
	O & M costs	\$120/year
	Replacement cost	\$350/kW
	Capital cost	\$400/kW
Converter	Type	3-phase
	Efficiency	95.5%
	Life time	16 years
	O & M cost	\$60/year
	Grid voltage & frequency	415 VAC 50/60 Hz
	Capital cost	\$320/kW
Battery	Type	Surrette 6CS25P
	O & M cost	\$100/year
	Replacement cost	\$1000/Battery
	Capital cost	\$1200/Battery
	Nominal energy capacity of each battery	6.94 kW
	Round trip efficiency	80%
	Minimum state of charge	40%
	Nominal capacity	1156 Ah (×1000 Batteries)
	Nominal Voltage	6 V (12 V for 2 batteries per string)
Wind	Minimum load ratio	30%
	Life	15 years
	O & M cost	\$1000/year
	Replacement cost	V82- \$1616660/turbine; V90 \$3060000/turbine
	Capital cost	V82- \$1716660/turbine; V90 \$3060000/turbine \$1716660/turbine
Grid	Price of electricity	\$0.032/kWh

components used in the HOMER simulations. The costs of the wind turbines and PV arrays are based on predicted prices for the year 2014.[49] The replacement cost for a V82 turbine was assumed to be lower since it is an older model, while that of V90 was assumed to remain constant. The PV arrays were assumed to not need replacement since their operating life is 25 years, which was equal to the project period.

V. RESULTS AND DISCUSSION

A. Wind rose plots and wind direction analysis

Figure 8 shows the wind rose plot for Yanbu, where the prevailing wind was from the northwest at 320°. This means that a wind turbine with a horizontal axis could be installed facing this direction to harvest the maximum wind energy. The calmest wind speeds were from the southeast at a speed of 0.5 m/s but only accounted for 2.1% of the observations.

The wind speed frequency distribution for Yanbu is shown in Fig. 9. The greatest frequency (24.3%) was for wind speeds of 3.5–5.0 m/s. Wind speeds above 3.5 m/s accounted for 51.2% of observations. The maximum wind speed was 10 m/s, which is well below the cut-out speed of the selected wind machines. This means that V82 and V90 wind turbines (each with a cut-in speed of 3.5 m/s) can be operated within this range.

Figure 10 shows the wind direction distribution for Yanbu. The prevailing wind direction was from 320° to 300° (NW). The least common wind direction was 160° (SE).

Figure 11 shows the wind rose plot for Dhahran. The prevailing wind was from the northwest at 330°. The calmest winds were from the southwest and only comprised 0.81% of the data. The maximum wind speed was 13.2 m/s which is greater than the 10 m/s maximum observed for Yanbu.

Figure 12 shows the wind speed frequency distribution for Dhahran. The wind speed was most commonly between 3.5 and 5 m/s (28.7% of observations). Wind speeds above 3.5 m/s accounted for 60.12% of the data, which is higher than Yanbu's proportion of 51.2%.

Figure 13 shows the wind directions for Yanbu. The prevailing wind direction was 330° followed by 0° (north) and 300°. The least common direction was 210° which is approximately SW.

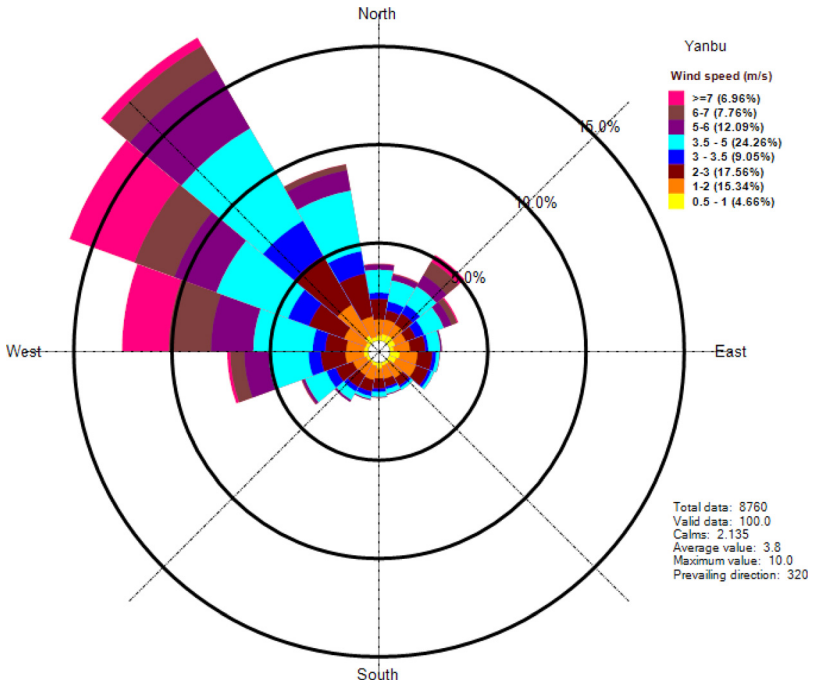

FIG. 8. Wind rose plot of winds at an elevation of 10 m (Yanbu).

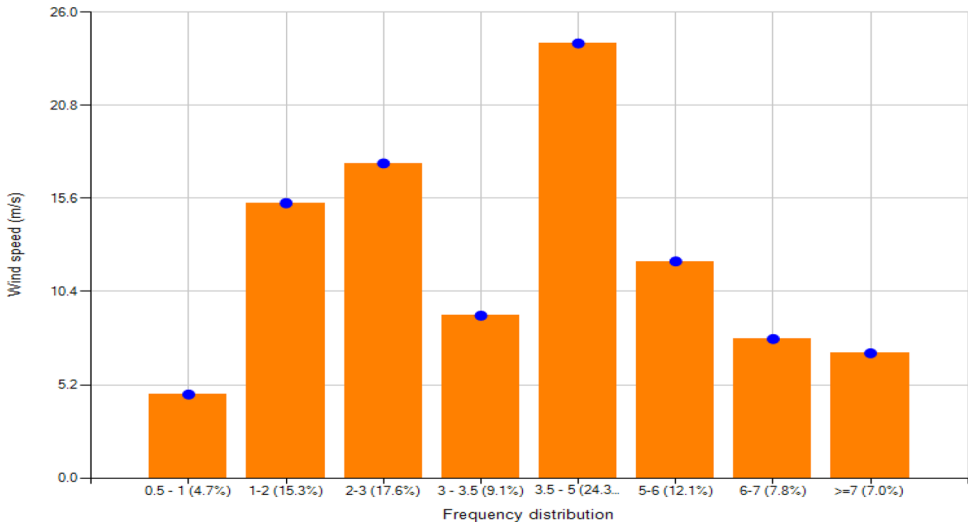

FIG. 9. Wind speed frequency distribution (Yanbu).

In general, it can be concluded that both locations have reasonable amounts of wind that could be used to operate the selected turbines. However, wind turbines with a cut-in speed of 3 m/s could harvest more power as the wind speed of 3 m/s was common (9.1% and 10.3% of the wind for Yanbu and Dhahran, respectively). Overall, wind speeds at Dhahran were higher than those at Yanbu.

B. Grid-connected hybrid wind/PV system analysis

Electrical output from the utilization of wind energy and solar energy was analyzed using the two hybrid system configurations in Fig. 14. From Fig. 14, the only visible difference between Figs. 14(a) and 14(b) is the wind turbines (Vestas V82 and Vestas V90 models). However, the same systems were utilized for each location, along with local wind and solar data.

1. Sensitivity analysis

Before concentrating on electrical output and cost analysis, it is important to discuss how the optimal systems were obtained from the simulation. Table IV shows the search space

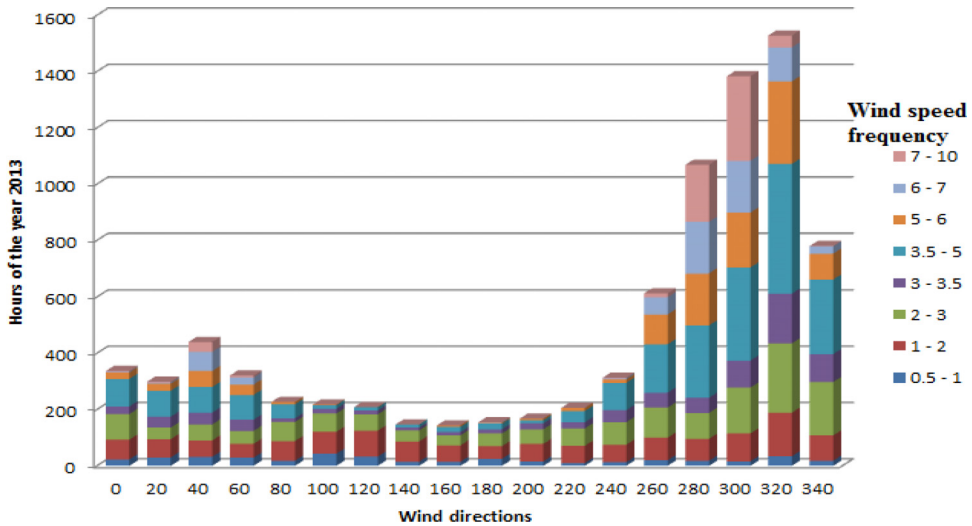

FIG. 10. Wind direction distribution (Yanbu).

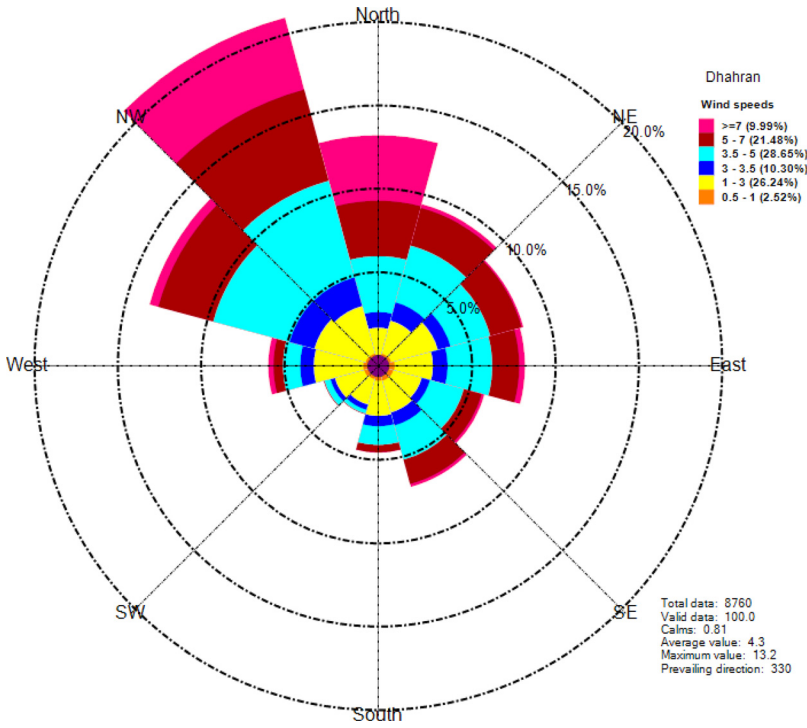

FIG. 11. Wind rose plot of winds at an elevation of 10 m (Dhahran).

specified for the sensitivity analysis of each component as it is fed into HOMER software. For each of the locations (Yanbu or Dhahran), the same search options were specified, but as seen in Table IV, different optimal results were obtained. The results discussed in Sec. V B 1 are based on the optimal results presented in Table IV.

For both locations, the minimum number of turbines was set at 3. This was done to ensure that the wind resource was not eliminated (by setting the minimum to zero) since this study is intended to assess the performance of the wind resource through the application of wind/PV hybrid systems. Optimal results with the Vestas V82 model were 6 turbines for Yanbu and 15 for Dhahran. In both cases, the search space was limited to 15 turbines. The main reason for obtaining 6 turbines at Yanbu lies in two factors: the available wind energy in this location and

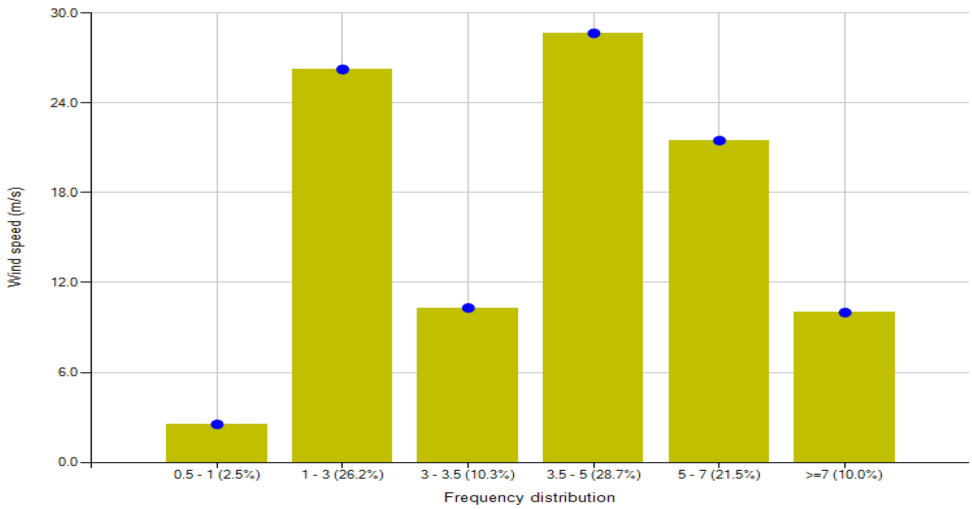

FIG. 12. Wind speed frequency distribution (Dhahran).

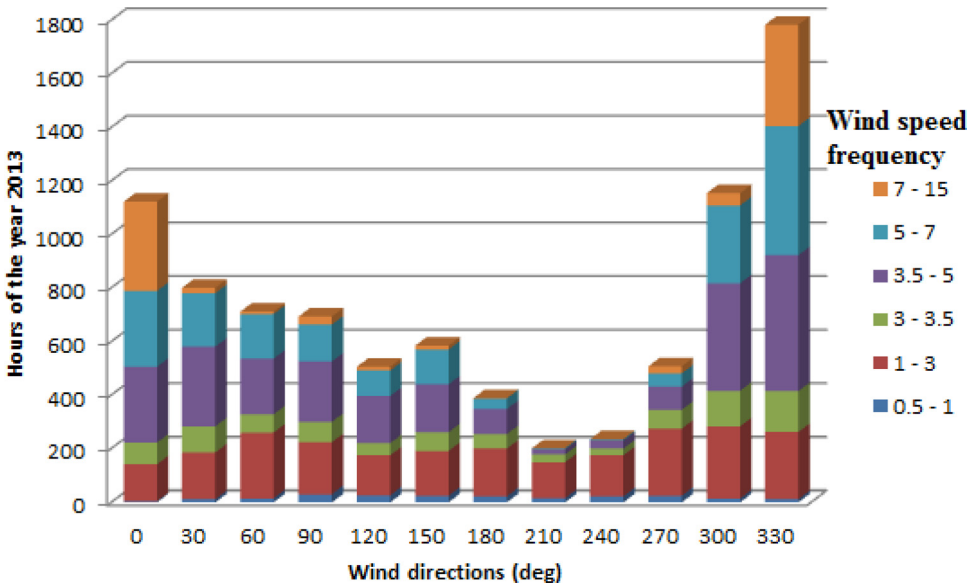

FIG. 13. Wind directional distribution for Dhahran.

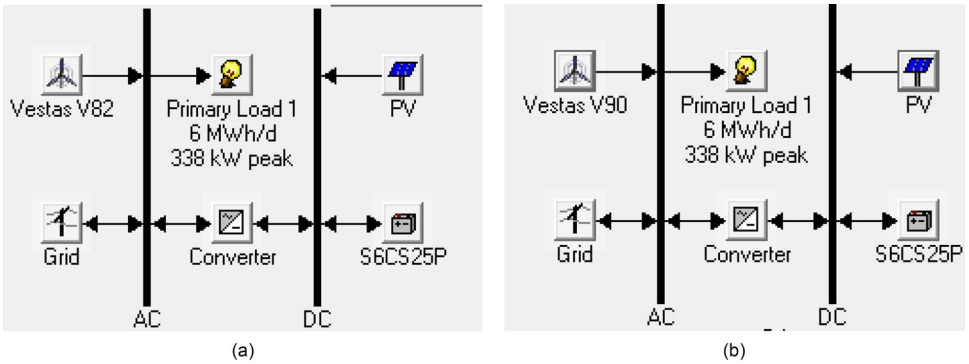

FIG. 14. System configuration for wind turbines: (a) Vestas V82 and (b) Vestas V90.

the cost of the turbines. It has already been observed that the wind energy for Dhahran exceeds that of Yanbu. The same unit costs of wind turbines were specified for both locations, with the only differentiating factor being wind energy availability. Therefore, because of lesser wind energy being available at Yanbu, the use of 6 Vestas V82 turbines was found to be optimal, somewhat less than the 15 turbines obtained for Dhahran. In this case, it can be noted that more wind energy

TABLE IV. Search space specified for sensitivity analysis.

System component (Units)	Search space	Optimal solution
Vestas V82 Wind turbine (number of turbines)	3, 4, 5, 6, 7, 8, 9, 10, 11, 12, 13, 14, 15	Yanbu: 6, Dhahran: 15
Vestas V90 Wind turbine (number of turbines)	3, 4, 5, 6, 7, 8, 9, 10, 11, 12, 13, 14, 15	3 (for both)
PV array (size, kW)	1000, 2000, 3000, 4000, 5000	1000 (for both)
Converter (size, kW)	1000, 2000, 3000, 4000, 5000	1000 (for both)
Surrette 6CS25P battery (number of batteries)	0, 50, 100, 200, 300, 500	0 (for the system without storage) or 50 (for the system with storage)

can be harvested at Dhahran than at Yanbu. However, because 15 Vestas V82 turbines produce a much higher electrical output with a large excess of electricity than the 6 turbines at Yanbu, a maximum of 6 turbines was set for Dhahran to enable a fair comparison. This also eliminated excess electricity which could not be sold to the grid as a cap is specified for grid sales.

For Vestas V90 models, 3 turbines were the optimal solution for both locations. This is attributed to the high cost of these turbines which has overpowered the wind energy availability constraint since cost is also specified as a constraint in the simulation.

The minimum and maximum sizes specified for the PV array and converter were 1000 kW and 5000 kW, respectively. In both cases, 1000 kW was obtained as the optimal solution for both locations. This means that a smaller size PV array was selected compared to systems using V82 turbines (6×1650 kW) and V90 wind turbines (3×3000 kW). One reason is that the wind resources in both locations were more suitable for power generation than solar resources. Another reason is that the PV arrays were more expensive in this case because of the added cost of the converters, while the turbines produce AC power which can be supplied directly to the load or grid.

Because of the presence of the grid, a small battery or none at all was used for storage. A maximum of 500 batteries were specified in the search space. A smaller storage capacity of 50 batteries was selected to compensate for capacity shortage and a small amount of unmet load, as discussed in Sec. V C.

C. Electrical analysis

For Yanbu, the monthly average electrical energy production by Vestas V82- and Vestas V90-based hybrid systems is indicated in Fig. 15. Both systems would have a constant PV power output of 1000 kW for all months, but wind power output and grid purchases were variable between months. The maximum electrical energy was generated in July because this was the month with the maximum wind speeds (Fig. 3), whereas the minimum was produced in November which had low wind speeds. Table V shows the estimated annual electrical energy production and consumption for both cases for Yanbu. For the grid-connected Vestas V82/PV system, the total annual energy production and consumption were about 12.60 GWh and 12.39 GWh, respectively. The small difference between production and consumption was due to

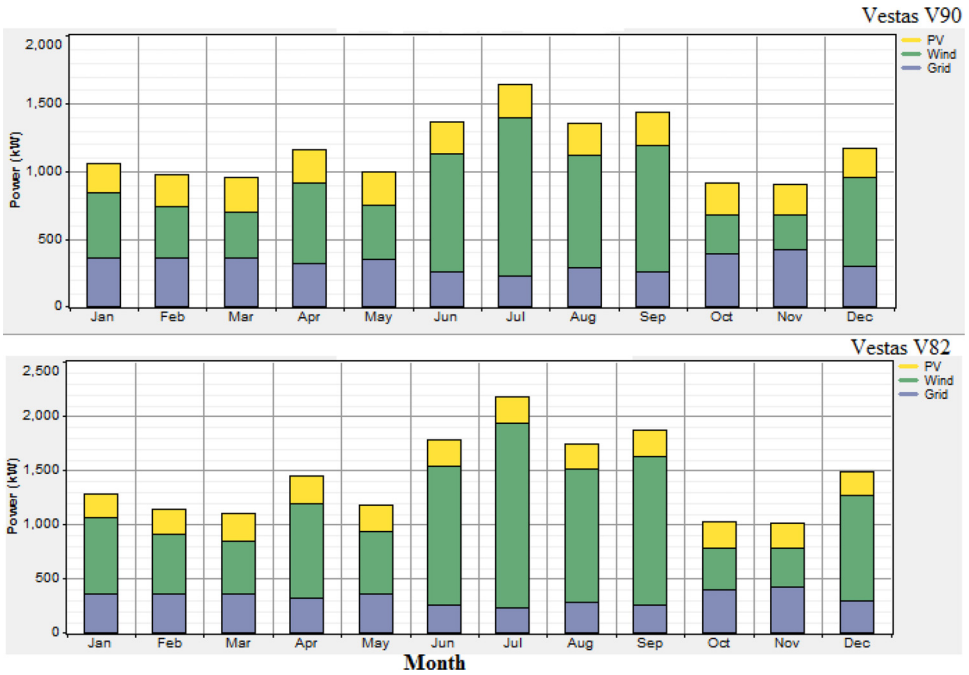

FIG. 15. Average monthly electrical power production for Yanbu using a V90-based system (above) and a V82-based system (below).

TABLE V. Annual energy distribution for Yanbu for the systems without batteries (no B).

	With Vestas V82		With Vestas V90	
Component	Annual Energy production (kWh) (no B)	Percentage (%)	Annual Energy production (kWh) (no B)	Percentage (%)
PV array	2 087 569	17	2 087 569	21
Wind turbines	7 650 805	61	5 257 892	52
Grid purchases	2 864 090	23	2 827 510	28
Total	12 602 463	100	10 172 971	100
	Annual Energy Consumption (kWh)		Annual Energy Consumption (kWh)	
AC primary load	6 570 106	52.13	6 570 106	64.58
Grid sales	5 823 590	46.21	3 394 095	33.36
Excess energy	9.35	0.00007	9.35	0.00009
Unmet load	0.00401	0	0.00482	0
Capacity shortage	265	0.0021	235	0.0023
Total	12 393 970	98.35	9 964 445	97.95
Error	208 493	1.65	208 526	2.05

excess electricity, unmet electrical load, and capacity shortages, being 9.35 kWh/year, 0.004 kWh/year, and 265 kWh/year, respectively, in addition to other losses. The capacity shortage was only recorded when there was no storage in the system. However, 50 batteries were used in parallel, and the capacity shortage reduced to zero. The error indicated in the last row of Table V represents the "other losses" between production and consumption. In power system analysis, losses exist during the transmission of electricity from the point of production to the point of consumption. In this case, since these losses were not stated in the software used, it is assumed that the losses were due to inefficiency in the software.

Since less energy is generated from a V90 turbine in a grid-connected V90/PV system, the production share of PV increased to 21%, up from a 17% share in a grid-connected V82/PV system. This is because V90 wind turbines are more expensive than V82 models, and hence, only 3 of them could be afforded in the model, instead of 6 V82 wind turbines. Electrical energy sales to the grid were 33.36% of production when V90 wind turbines were used, while V82 systems could sell 46.21%.

Figure 16 shows the monthly average electrical power production for Dhahran. The maximum and minimum production occurred in June and November, when wind speeds were maximal and minimal, respectively. The annual energy distribution for Dhahran is shown in Table VI for systems without batteries. The PV output power remained at 1000 kW for both grid-connected V82/PV and grid-connected V90/PV systems. However, the PV energy production share increased to 18% when V90 systems were used, up from 14% with V82 systems. Grid purchases also increased from 17% to 22% due to the increased hours of use for the grid energy with the power purchase limit being still maintained at 1000 kW. This was also due to the reduced amount of wind energy (from 69% to 60%) harvested with V90 systems. Likewise, grid energy sales declined from 52.44% to 38.94%.

D. Grid energy distribution

The seasonal grid energy distribution for Yanbu is shown in Fig. 17 and comprises energy sold to the grid, energy purchased from the grid, and net energy purchases. With Vestas V82 systems [Fig. 17(a)], the annual energy purchases from the grid for the systems both with and without storage were 2 864 090 kWh. The annual energy purchases are the same in both cases because seasonal energy distribution is the same for each month, and therefore, the two curves

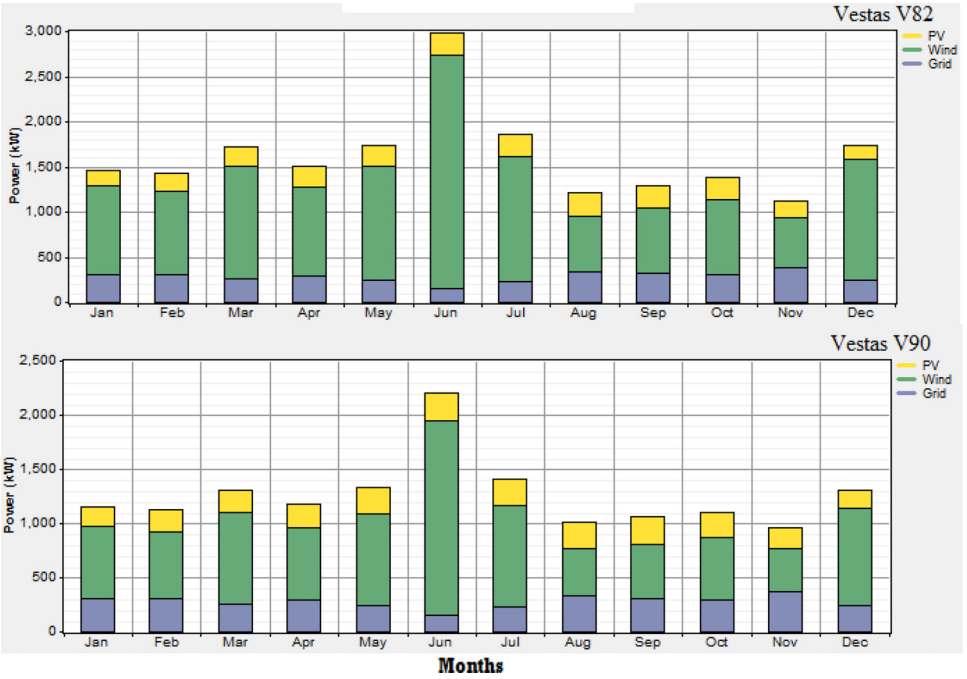

FIG. 16. Average monthly electric production for Dhahran using a V82-based system (above) and a V90-based system (below).

overlap in Fig. 17. The respective energy sales to the grid with and without batteries were 3 394 095 kWh and 5 823 590 kWh, respectively.

The grid energy distribution for Dhahran is shown in Fig. 18. It can be observed in both Figs. 18(a) and 18(b) that the energy purchased, energy sold, and net purchase without batteries (no B) were the same as the respective energy purchased, energy sold, and net purchase with batteries (with B). This is because the small storage capacity of 50 batteries was only used to cover the capacity shortage but did not affect the amount of energy sold and purchased from

TABLE VI. Annual energy distribution for Dhahran: systems without batteries (no B).

	With Vestas V82		With Vestas V90	
Component	Annual Energy production (kWh) (no B)	Percentage (%)	Annual Energy production (kWh) (no B)	Percentage (%)
PV array	1 944 360	14	1 944 360	18
Wind turbines	9 806 135	69	6 677 203	60
Grid purchases	2 473 902	17	2 457 229	22
Total	14 224 397	100	11 078 791	100
	Annual Energy Consumption (kWh)		Annual Energy Consumption (kWh)	
AC primary load	6 570 014	46.19	6 570 014	59.30
Grid sales	7 459 892	52.44	4 314 330	38.94
Excess energy	26	0.00018	26	0.00023
Unmet load	0	0	0	0
Capacity shortage	308	0.0022	237	0.0021
Total	14 030 240	98.64	10 884 607	98.25
Error	194 157	1.36	194 184	1.75

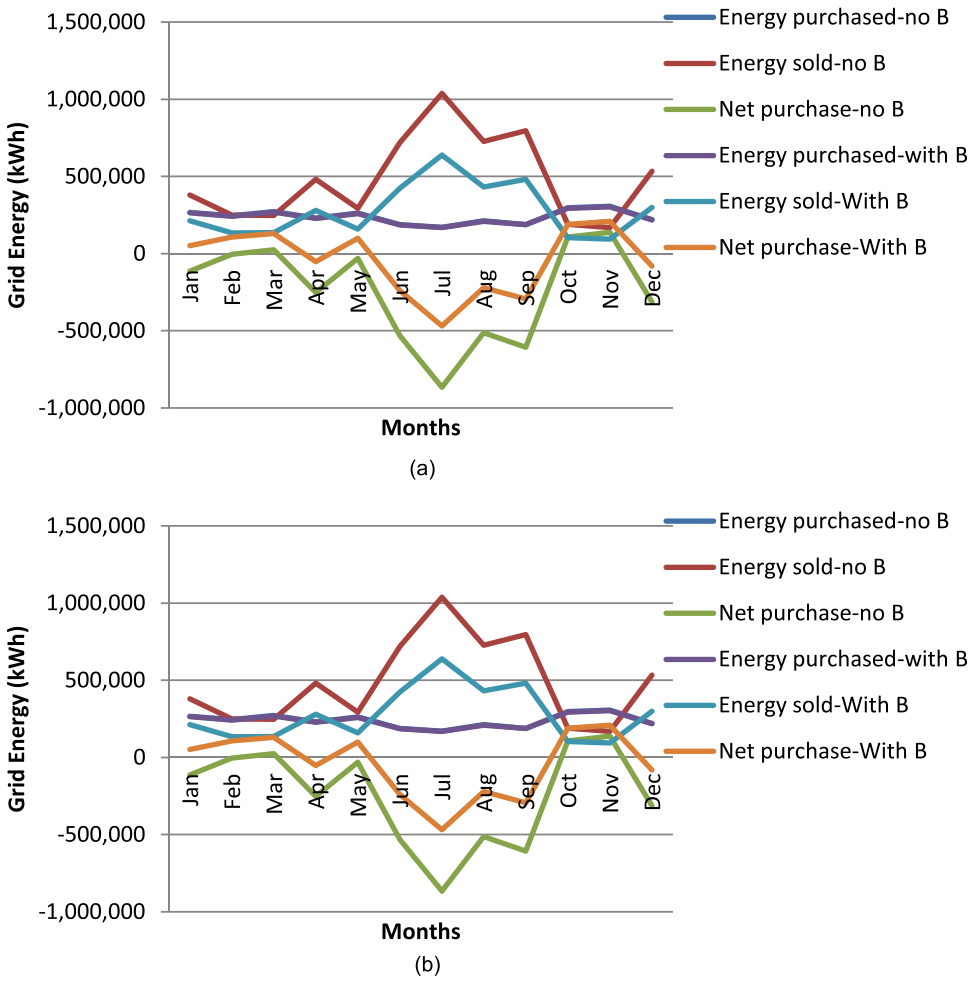

FIG. 17. Seasonal grid energy distribution for Yanbu: (a) Vestas V82 (b) Vestas V90.

the grid. Hence, the batteries in this case can be used to eliminate capacity shortages and prevent interruptions to the primary load.

E. Economic analysis

Economic analysis was based on NPC and the LCOE of each case that was needed for comparison. Beginning with Yanbu, Fig. 19 shows the NPC for each cost type when Vestas V82 wind turbines were present in a grid-connected wind/PV system. From Fig. 19(a), it is observed that the largest part of the NPC is dominated by capital and replacement costs of $11 079 960 and $9 558 650, respectively. The operating cost was negative, meaning that the system operator could sell excess energy to the grid. The salvage was also large because the wind system would be replaced after 15 years, meaning that by the end of the project period of 25 years, the value of the wind turbine replacement would still be high. Therefore, because of the financial gains from grid sales and a large portion of salvage, the total NPC would reduce to $15 572 176. There was no fuel used in this project; therefore, the value is indicated to be zero. Using a similar analysis, the total NPC for the system without storage was $15 456 008 [Fig. 19(b)]. In this case, when storage was used, the NPC increased by 0.75% compared to the system without storage. However, the increase in NPC in this case came with improved reliability and system power quality since the capacity shortage reduced to zero. Amjad *et al.*[50] noted that, considering environmental concerns and rapid socioeconomic growth, increased energy efficiency, energy independency, better power quality, and higher service reliability are important pursuits for many modern societies. Therefore,

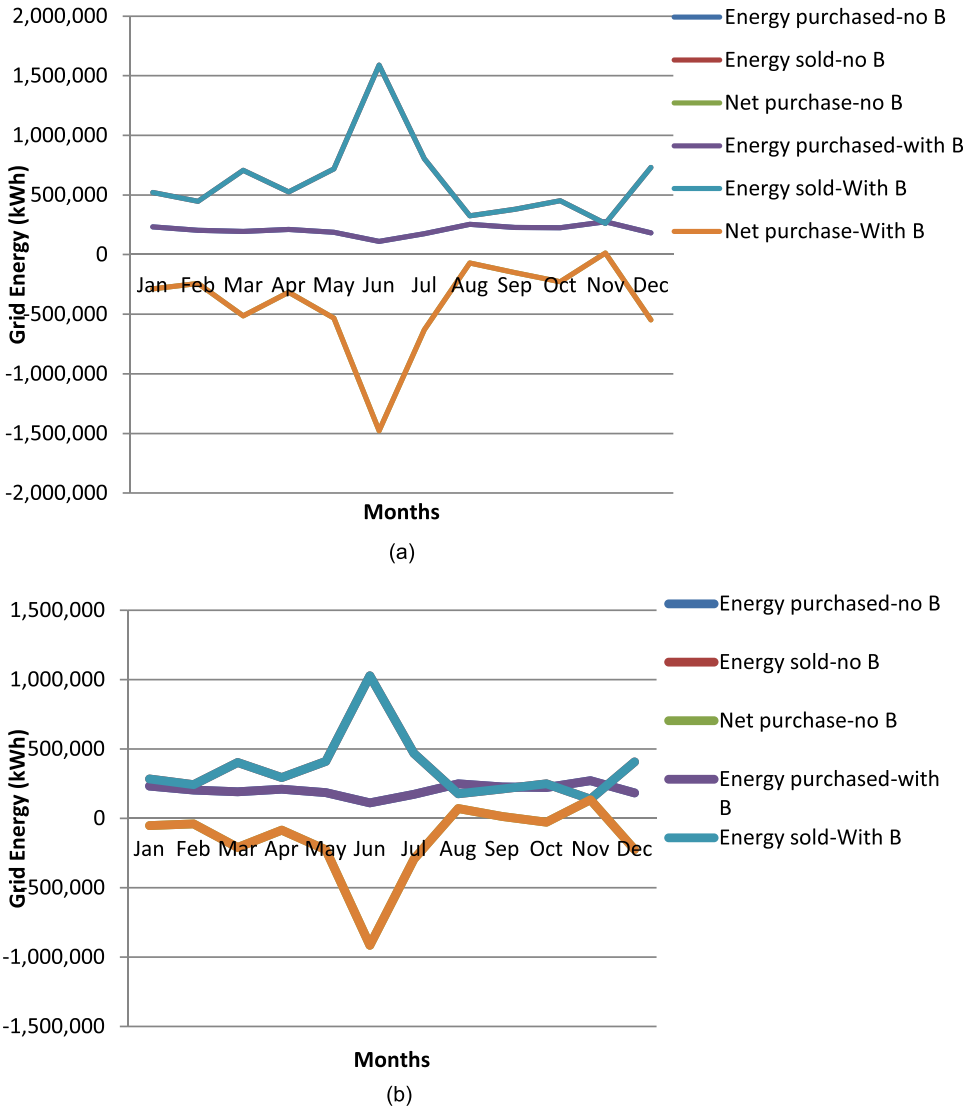

FIG. 18. Seasonal grid energy distribution for Dhahran: (a) Vestas V82 (b) Vestas V90.

increased cost of an energy system with a small storage capacity can be justified by the advantages that come with that system.

Figure 20 shows the NPC by the component type for grid-connected Vestas V82/PV systems with storage, at Yanbu. It is clear that the largest portion of NPC goes to the wind turbines (V82), while the batteries (S6CS25P) contribute the smallest portion. Other costs are incurred by the salvage of the system after the end of the project period.

For a grid-connected Vestas V90/PV system at Yanbu, capital and replacement costs still dominate NPC at \$9 900 000 and \$8 993 464, respectively (Fig. 21). Moreover, the total NPC was \$19 130 750, which was 23.8% higher than that of the grid-connected Vestas V82/PV system without storage. There are two main reasons for the cost difference. Given that PV power output and grid purchases were the same (1000 kW each) and assuming similar hours of operation and operating costs (\$1000/year), for a grid-connected Vestas V82/PV system, 6 V82 turbines were the optimal solution, giving $6 \times 1.65\,\text{MW} = 9.9\,\text{MW}$. Alternatively, for grid-connected Vestas V90/PV systems, 3 V90 turbines were the optimal solution and would produce $3 \times 3.0\,\text{MW} = 9.0\,\text{MW}$. Even with the V90 systems' lower power output (9.0 MW) than that of the V82 systems (9.9 MW), using 3 V90 wind turbines would result in higher NPC than with 6 V82-based systems. The main reason is the higher unit cost of V90 models.

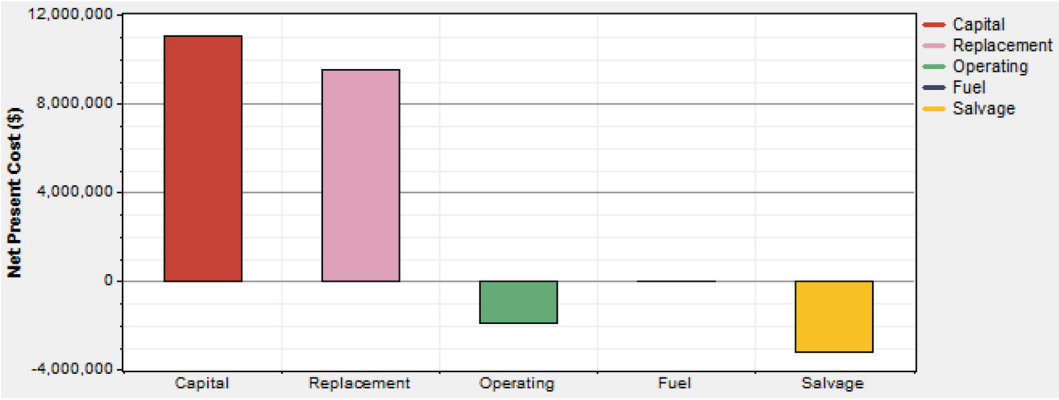

(a)

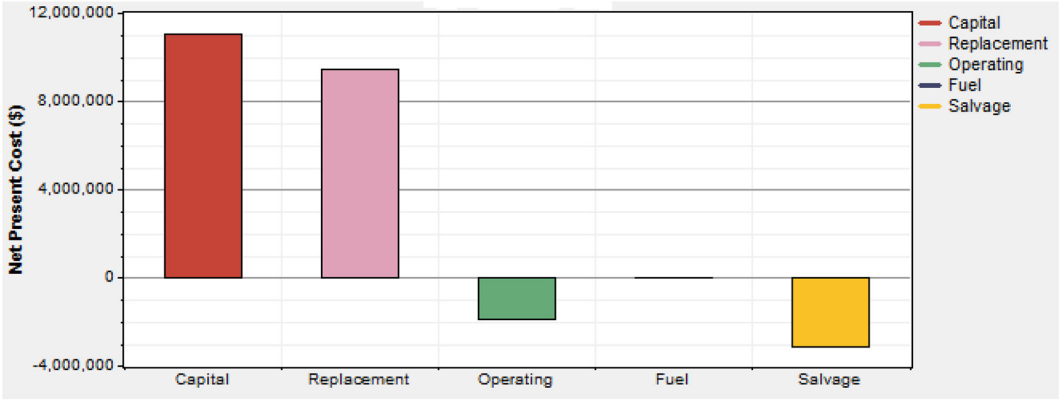

(b)

FIG. 19. Cash flow summary by the cost type for V82 wind turbines at Yanbu: (a) with batteries and (b) without batteries.

Similarly, in the case of systems using Vestas V90 turbines with batteries at Yanbu, the cost of batteries was very small compared to the cost of the other components. Nevertheless, the cost difference between systems with and without batteries is indicated in the total NPC of the whole system.

The LCOE for V82/PV systems without storage, V82/PV with storage, V90/PV without storage, and V90/PV with storage were \$0.054/kWh, \$0.054/kWh, \$0.083/kWh, and \$0.054/kWh, respectively. It is clear that the unit cost of energy produced with V90 systems would be very high. The inclusion of a small storage unit would not affect the LCOE of the system

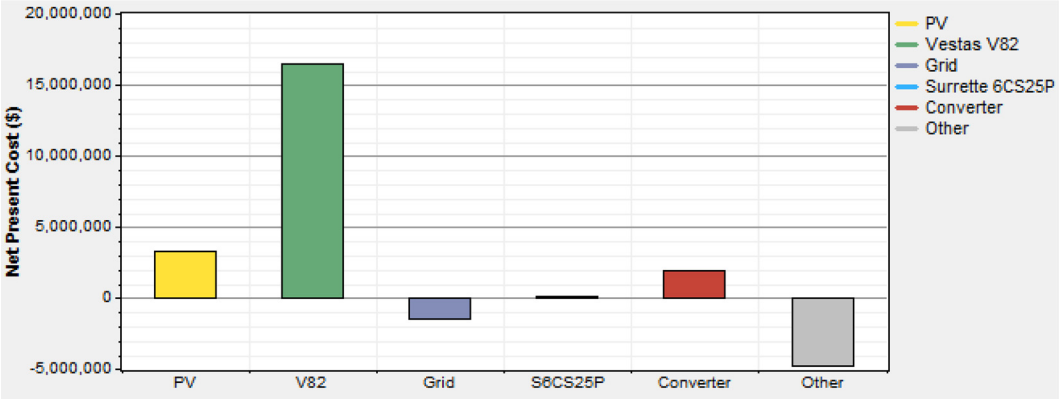

FIG. 20. Cash flow summary by the component type for V82 wind turbines with storage at Yanbu.

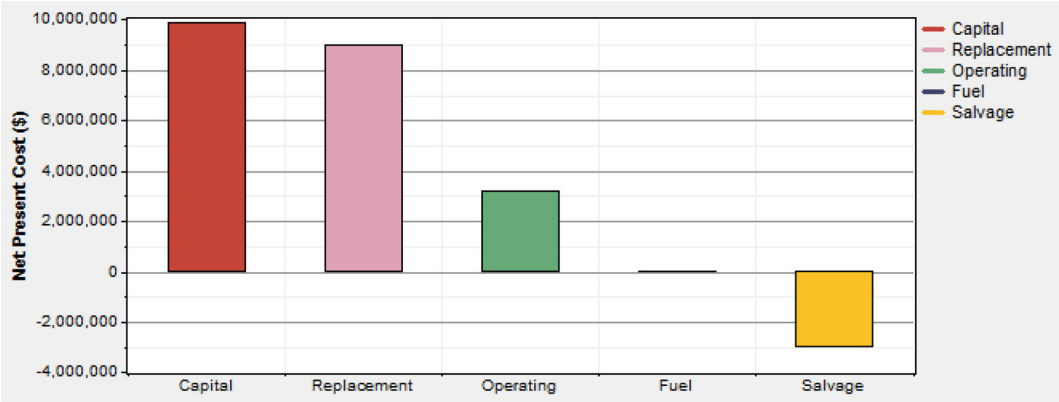

FIG. 21. Cash flow summary by the cost type for a grid-connected Vestas V90/PV system without storage.

although it would give the advantage of covering capacity shortages, ensuring uninterrupted supply.

A similar approach to that used for the Yanbu systems was used to model systems installed at Dhahran. Figure 22(a) shows the NPC of each cost type for a grid-connected V82/PV system with storage. Note that the capital and replacement costs for all system components used at Dhahran were the same as for Yanbu. The capital and replacement costs still compose the biggest share of NPC [Fig. 22(a)]. The operating cost was $-6 249 093, which was more expensive

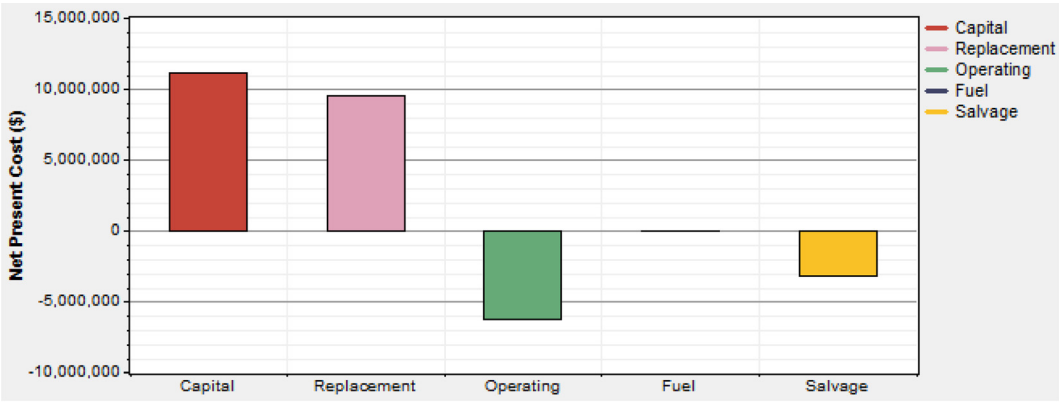

(a)

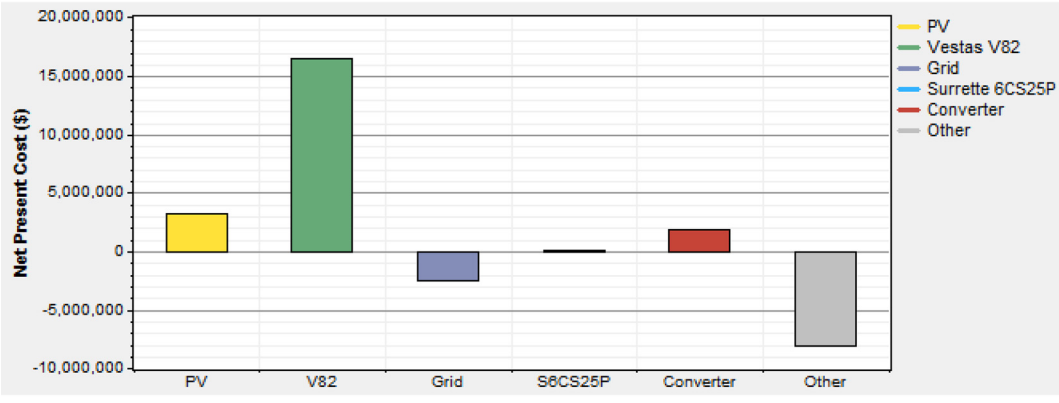

(b)

FIG. 22. Cash flow summary for a grid-connected V82/PV system with storage by (a) the cost type and (b) the component type.

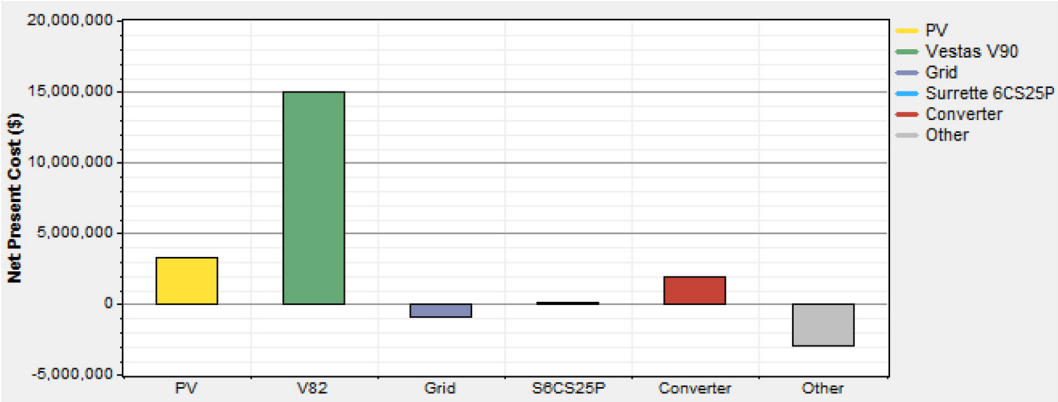

FIG. 23. NPC of each component for a grid-connected V90/PV system with batteries at Dhahran.

than that of a grid-connected V82/PV system at Yanbu ($-1 896 186). The values are negative, meaning that a relatively high amount of electricity was sold to the grid, raising some income for the system operator. The total NPC was $11 219 270, which was 38.7% less than that of a similar system at Yanbu (NPC = 15 572 176). However, the energy output from a grid-connected V82/PV system at Dhahran would be 14 224 397 kWh, which is 12.8% more than a similar system at Yanbu (12 602 463 kWh). This means that the application of a grid-connected hybrid V82/PV system at Dhahran would be cheaper than at Yanbu although the Dhahran system would generate a higher energy output. Moreover, the LCOE for a V82-based system at Dhahran was $0.035/kWh, which is less than that of a similar system at Yanbu ($0.054/kWh). The higher performance of systems at Dhahran was attributed to higher wind speeds. This results in more electricity production, some of which can be sold to the grid. As a result, energy unit costs are lower.

The estimated LCOEs were the same for grid-connected V82/PV systems with and without storage since batteries contributed a very small additional NPC [Fig. 22(b)]. The wind turbines are the dominant components in terms of NPC.

Figure 23 shows the NPC of each component in a grid-connected V90/PV system with batteries at Dhahran. The Vestas V90 turbines had high NPC values, while batteries had the

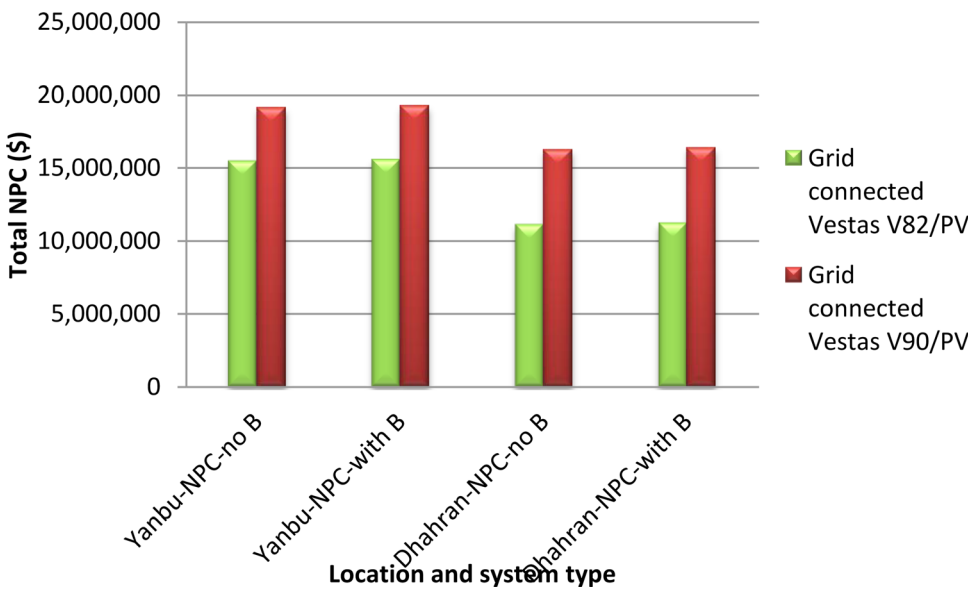

FIG. 24. Total NPC for each optimal configuration.

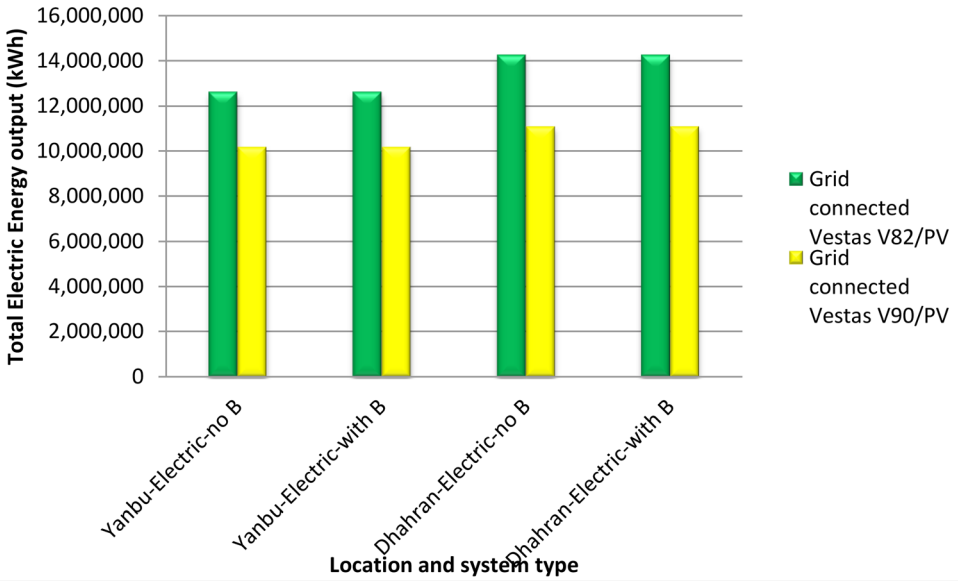

FIG. 25. Total electrical energy production from the optimal systems.

lowest. Like the same system at Yanbu, this system sold less energy to the grid but had a larger total NPC value ($16 380 500) as compared with the hybrid V82/PV system at Dhahran. This makes the unit cost of energy higher (LCOE of $0.065/kWh) compared with a V82-based system but still lower than that of a grid-connected V90/PV system at Yanbu.

Figure 24 shows the comparison of total NPC for all four optimal systems at both locations. Hybrid systems with V90 wind turbines had the highest NPC of all systems. As observed earlier, the system with V90 (maroon color) without batteries at Yanbu (Yanbu-NPC-no B) had the highest NPC, which was almost the same as the system with batteries (Yanbu-NPC-with B). Surprisingly, these systems with the highest NPC had the least total electrical energy output (Fig. 25). In contrast, V82-based systems at Dhahran had the lowest NPC and highest electrical energy output, as well as the least LCOE. Hence, a grid-connected Vestas V82/PV system was most economically viable of the four hybrid systems compared.

VI. CONCLUSION

The analysis of the electricity production potential and economic viability of grid-connected wind/PV hybrid energy systems has been conducted for two cities, Yanbu and Dhahran, located on the western and eastern coasts of Saudi Arabia. The results indicate that both locations have a sufficient amount of wind for operating the selected wind turbines. However, using wind turbines with a cut-in speed of 3 m/s could allow more power to be harvested, as a significant amount of wind with a wind speed of 3 m/s is available. Wind speeds at Dhahran were higher than at Yanbu with wind speeds above 3.5 m/s, accounting for 60.12% of the wind data at Dhahran, which is higher than 51.2% of Yanbu. It has been demonstrated that hybrid systems with Vestas V90 wind turbines have the highest NPC of all system configurations compared. In addition, V90 systems have been observed with the highest NPC at Yanbu, regardless of the inclusion of battery storage. Surprisingly, the system with the highest NPC is observed with the least total electrical energy output. In contrast, Vestas V82-based systems at Dhahran recorded the lowest NPC and LCOE but with the highest electrical energy output. Hence, a grid-connected Vestas V82/PV system is most economically viable of the four hybrid systems compared. It is recommended to incorporate a small battery storage unit in grid-connected wind/PV systems to minimize the capacity shortages and improve the system reliability although this comes at the expense of a slight increase in total system NPC. Therefore,

optimal sizing of hybrid system components is essential in order to serve all load demands with minimum energy cost and high reliability.

ACKNOWLEDGMENTS

This work was supported by the Deanship of Scientific Research (DSR), King Abdulaziz University, Jeddah, under Grant No. (135-25-D1437). The authors, therefore, gratefully acknowledge the DSR technical and financial support.

[1]A. B. Stambouli, Z. Khiat, S. Flazi, and Y. Kitamura, "A review on the renewable energy development in Algeria: Current perspective, energy scenario and sustainability issues," Renewable Sustainable Energy Rev. **16**(7), 4445–4460 (2012).
[2]D. O. Akinyele and R. K. Rayudu, "Community-based hybrid electricity supply system: A practical and comparative approach," Appl. Energy **171**, 608–628 (2016).
[3]E. D. Giannoulis and D. a. Haralambopoulos, "Distributed generation in an isolated grid: Methodology of case study for Lesvos—Greece," Appl. Energy **88**(7), 2530–2540 (Jul. 2011).
[4]EIA, see http://www.eia.gov for Overview Data for Saudi Arabia (last accessed 12 January 2014).
[5]M. A. M. Ramli, S. Twaha, and Z. Al-Hamouz, "Analyzing the potential and progress of distributed generation applications in Saudi Arabia: The case of solar and wind resources," Renewable Sustainable Energy Rev. **70**(2016), 287–297 (2017).
[6]S. M. Rahman and a. N. Khondaker, "Mitigation measures to reduce greenhouse gas emissions and enhance carbon capture and storage in Saudi Arabia," Renewable Sustainable Energy Rev. **16**(5), 2446–2460 (2012).
[7]V. Tola and A. Pettinau, "Power generation plants with carbon capture and storage: A techno-economic comparison between coal combustion and gasification technologies," Appl. Energy **113**, 1461–1474 (2014).
[8]J.-H. Wee, "A review on carbon dioxide capture and storage technology using coal fly ash," Appl. Energy **106**, 143–151 (2013).
[9]O. Ellabban, H. Abu-Rub, and F. Blaabjerg, "Renewable energy resources: Current status, future prospects and their enabling technology," Renewable Sustainable Energy Rev. **39**, 748–764 (2014).
[10]A. Hepbasli and Z. Alsuhaibani, "A key review on present status and future directions of solar energy studies and applications in Saudi Arabia," Renewable Sustainable Energy Rev. **15**(9), 5021–5050 (Dec. 2011).
[11]C. Wang, S. S. Member, M. H. Nehrir, and S. S. Member, "Analytical approaches for optimal placement of distributed generation sources in power systems," IEEE Trans. Power Syst. **19**(4), 2068–2076 (2004).
[12]S. J. Mirazimi, M. Nematollahi, M. H. Ashourian, and S. Mirahmadi, "Reconfiguration and DG placement considering critical system condition," in *IEEE 7th International Power Engineering and Optimization Conference (PEOCO)* (2013), pp. 676–679.
[13]S. Bhattacharjee and S. Acharya, "Performative analysis of an eccentric solar-wind combined system for steady power yield," Energy Convers. Manage. **108**, 219–232 (2016).
[14]K. J. Chua, W. M. Yang, S. S. Er, and C. Ho, "Sustainable energy systems for a remote island community," Appl. Energy **113**, 1752–1763 (2014).
[15]S. Sinha and S. S. Chandel, "Review of recent trends in optimization techniques for solar photovoltaic-wind based hybrid energy systems," Renewable Sustainable Energy Rev. **50**, 755–769 (2015).
[16]S. Sinha and S. S. Chandel, "Improving the reliability of photovoltaic-based hybrid power system with battery storage in low wind locations," Sustainable Energy Technol. Assess. **19**, 146–159 (2017).
[17]M. Qolipour, A. Mostafaeipour, S. Shamshirband, O. Alavi, H. Goudarzi, and D. Petković, "Evaluation of wind power generation potential using a three hybrid approach for households in Ardebil Province, Iran," Energy Convers. Manage. **118**, 295–305 (2016).
[18]A. Hiendro, R. Kurnianto, M. Rajagukguk, Y. M. Simanjuntak, and Junaidi, "Techno-economic analysis of photovoltaic/wind hybrid system for onshore/remote area in Indonesia," Energy **59**, 652–657 (2013).
[19]G. Rohani and M. Nour, "Techno-economical analysis of stand-alone hybrid renewable power system for Ras Musherib in United Arab Emirates," Energy **64**, 828–841 (2014).
[20]G. Bekele and G. Tadesse, "Feasibility study of small Hydro/PV/Wind hybrid system for off-grid rural electrification in Ethiopia," Appl. Energy **97**, 5–15 (2012).
[21]O. Hafez and K. Bhattacharya, "Optimal planning and design of a renewable energy based supply system for microgrids," Renewable Energy **45**, 7–15 (2012).
[22]G. Bekele and B. Palm, "Feasibility study for a standalone solar-wind-based hybrid energy system for application in Ethiopia," Appl. Energy **87**(2), 487–495 (2010).
[23]F. Baghdadi, K. Mohammedi, S. Diaf, and O. Behar, "Feasibility study and energy conversion analysis of stand-alone hybrid renewable energy system," Energy Convers. Manage. **105**, 471–479 (2015).
[24]Y. Himri, A. S. Malik, A. Boudghene Stambouli, S. Himri, and B. Draoui, "Review and use of the Algerian renewable energy for sustainable development," Renewable Sustainable Energy Rev. **13**(6–7), 1584–1591 (2009).
[25]S. Twaha, M. H. Idris, M. Anwari, and A. Khairuddin, "Applying grid-connected photovoltaic system as alternative source of electricity to supplement hydro power instead of using diesel in Uganda," Energy **37**(1), 185–194 (2012).
[26]S. Twaha, M. A. M. Ramli, P. M. Murphy, M. U. Mukhtiar, and H. K. Nsamba, "Renewable based distributed generation in Uganda: Resource potential and status of exploitation," Renewable Sustainable Energy Rev. **57**, 786–798 (2016).
[27]L. M. Al-Hadhrami, "Performance evaluation of small wind turbines for off grid applications in Saudi Arabia," Energy Convers. Manage. **81**, 19–29 (2014).
[28]M. A. Baseer, J. P. Meyer, M. M. Alam, and S. Rehman, "Wind speed and power characteristics for Jubail industrial city, Saudi Arabia," Renewable Sustainable. Energy Rev. **52**, 1193–1204 (2015).

[29]S. Rehman and A. Z. Sahin, "Wind power utilization for water pumping using small wind turbines in Saudi Arabia: A techno-economical review," Renewable Sustainable Energy Rev. **16**(7), 4470–4478 (2012).
[30]S. Rehman, I. M. El-amin, F. Ahmad, S. M. Shaahid, A. M. Al-shehri, and J. M. Bakhashwain, "Wind power resource assessment for Rafha, Saudi Arabia," Renewable Sustainable Energy Rev. **11**, 937–950 (2007).
[31]H. El Khashab and M. Al Ghamedi, "Comparison between hybrid renewable energy systems in Saudi Arabia," J. Electr. Syst. Inf. Technol. **2**(1), 111–119 (2015).
[32]S. Rehman and L. M. Al-Hadhrami, "Study of a solar PV–diesel–battery hybrid power system for a remotely located population near Rafha, Saudi Arabia," Energy **35**(12), 4986–4995 (2010).
[33]M. A. Mohandes, "Modeling global solar radiation using particle swarm optimization (PSO)," Sol. Energy **86**(11), 3137–3145 (2012).
[34]M. Benghanem and A. Mellit, "Radial Basis Function Network-based prediction of global solar radiation data: Application for sizing of a stand-alone photovoltaic system at Al-Madinah, Saudi Arabia," Energy **35**(9), 3751–3762 (2010).
[35]M. A. M. Ramli, S. Twaha, and Y. A. Al-Turki, "Investigating the performance of support vector machine and artificial neural networks in predicting solar radiation on a tilted surface: Saudi Arabia case study," Energy Convers. Manage. **105**, 442–452 (2015).
[36]A. Kaabeche, M. Belhamel, and R. Ibtiouen, "Sizing optimization of grid-independent hybrid photovoltaic/wind power generation system," Energy **36**(2), 1214–1222 (2011).
[37]GIS, see https://solargis.info/purchase/#tl=Google:hybrid&bm=satellite&loc=24.023176,38.189978&c=24.023176,38.189978&z=15&ot=CLIMDATA for GIS solar and wind data.
[38]S. Rehman and N. M. Al-abbadi, "Wind shear coefficients and energy yield for Dhahran, Saudi Arabia," Renewable Energy **32**, 738–749 (2007).
[39]Enviroware, see http://www.enviroware.com/portfolio/windrose-pro3/ for WindRose PRO3 Overview (last accessed 01 October 2014).
[40]D. L. Elliott, C. G. Holladay, W. R. Barchet, H. P. Foote, and W. F. Sandusky, *Wind Energy Resource Atlas of the United States* (Taylor & Francis Group, LLC, 2006), p. 44.
[41]C. G. Justus, "Wind energy statistics for large arrays of wind turbines (New England and Central U.S. Regions)," Sol. Energy **20**(5), 379–386 (1978).
[42]International Electrotechnical Committee IEC 61400–1. *Wind Turbines. Part 1: Design Requirements*, 3rd ed. (IEC, Geneva, Switzerland, 2005).
[43]International Electrotechnical Committee IEC. 61400–3. *Wind Turbines. Part 3: Design Requirements for Offshore Wind Turbines*, 1st ed. (IEC, Geneva, Switzerland, 2009).
[44]see www.homerenergy.com/microgrid-power-system-design-services.html for Microgrid Power System Design Services Using HOMER.
[45]M. A. M. Ramli, A. Hiendro, K. Sedraoui, and S. Twaha, "Optimal sizing of grid-connected photovoltaic energy system in Saudi Arabia," Renewable Energy **75**, 489–495 (Mar. 2015).
[46]M. A. M. Ramli, A. Hiendro, and S. Twaha, "Economic analysis of PV/diesel hybrid system with flywheel energy storage," Renewable Energy **78**, 398–405 (2015).
[47]S. Twaha and M. U. Mukhtiar, "Optimal hybrid renewable-based distributed generation system with feed-in tariffs and ranking technique," in *The 2014 IEEE International Power Engineering and Optimization Conference (PEOCO2014)* (2014), pp. 115–120.
[48]Dynamic Energy & Water Solutions, see http://www.dynamic-ews.com/Tariffs/Electricity%20Tariffs/KSA.pdf for Kingdom of Saudi Arabia Electricity Tariffs, 2001.
[49]Wind Power, see http://www.windpowermonthly.com/article/1117015/turbine-prices-fall-until-2014 for Turbine prices could fall until 2014, 2011.
[50]A. A. Moghaddam, A. Seifi, T. Niknam, and M. R. Alizadeh Pahlavani, "Multi-objective operation management of a renewable MG (micro-grid) with back-up micro-turbine/fuel cell/battery hybrid power source," Energy **36**(11), 6490–6507 (2011).